# Novel methods of constraining the parton distribution function uncertainty in the measurement of the W-boson mass

Ashutosh V. Kotwal

Phys. Rev. D **98**, 033008 — Published 30 August 2018

DOI: 10.1103/PhysRevD.98.033008

# Novel methods of constraining the parton distribution function uncertainty in the measurement of the $W$-boson mass

Ashutosh V. Kotwal[1]

[1]*Department of Physics, Duke University, Durham, North Carolina 27708, USA*

The measurement of the mass of the $W$ boson is one of the most precise and impactful measurements to test the standard model (SM). Following the discovery of the Higgs boson and the measurement of its mass, all SM parameters are sufficiently well-known in order to make precise predictions for electroweak observables such as the $W$ boson mass. These observables receive corrections in extensions of the SM. Experimentally, the dominant uncertainty in the $W$-boson mass measurement at hadron colliders arises due to parton distribution functions (PDFs). We present novel *in situ* methods of constraining the PDF variation and of reducing the PDF impact on the $W$-mass measurement uncertainty at hadron colliders. These methods can exploit the very high-statistics samples of $W$-boson candidate events at the LHC.

PACS numbers: 12.15.-y, 12.15.Ji, 13.38.Be, 13.85.Qk, 14.70.Fm

The discovery [1] of the Higgs boson in 2012 has confirmed the Higgs mechanism [2] of the standard model [3] for generating masses for the electroweak gauge bosons. The Yukawa couplings between the Higgs field and some of the fermions have also been observed. Even so, the Higgs sector of the standard model (SM) continues to contain riddles. The Higgs potential in the SM is empirical without a dynamical or symmetry-based explanation. The values of the fermion Yukawa couplings vary widely between generations. Finally, unlike other dimensionless SM parameters which are multiplicatively renormalized and depends logarithmically on the ultraviolet cutoff, the dimensionful parameter that defines the observable Higgs boson mass and the field's vacuum expectation value is additively renormalized with a quadratic dependence on the ultraviolet cutoff. This leads to the well-known "fine-tuning" problem of the Higgs boson mass if there is a large hierarchy between the electroweak scale and the energy scale of new physics, eg. the Planck scale. To render the Higgs potential parameters "natural", it has been postulated that new physics should provide an ultraviolet cutoff for loop diagrams that is not much higher than the electroweak scale.

As the Higgs boson mass $M_H$ is parametrically defined, its value was historically constrained by measurements of the weak-boson masses and other precision electroweak observables through the Higgs-loop induced corrections. For example, loops in the $W$-boson propagator contribute to the correction $\Delta r$, defined in the following expression for the $W$-boson mass $M_W$ in the *on-shell* scheme [4]:

$$M_W^2 = \frac{\hbar^3 \pi}{c} \frac{\alpha_{EM}}{\sqrt{2} G_F (1 - M_W^2/M_Z^2)(1 - \Delta r)}, \qquad (1)$$

where $\alpha_{EM}$ is the electromagnetic coupling at $Q = M_Z c^2$, $G_F$ is the Fermi weak coupling extracted from the muon lifetime, $M_Z$ is the $Z$-boson mass, and $\Delta r = 3.58\%$ [5] includes all radiative corrections. $\Delta r$ is dominated by quark loops while depending logarithmically on $M_H$. The directly-measured $M_H$ is consistent with the fit to the electroweak observables, where the fit precision is dominated by the uncertainty on $M_W$ and the weak mixing angle, with smaller contributions from the uncertainties on the top quark mass and $\alpha_{EM}$.

The direct measurement of $M_H$ enables precise predictions for the precision electroweak observables at the level of 0.01%. Measuring these observables at this level of precision provides a stringent test of new physics through loop effects [6]. A discrepancy between the measured and predicted values of $M_W$ can be interpreted in the framework of effective field theory as a measurement of the energy scale of new physics. Evidence of physics beyond the SM would be revolutionary for the advancement of fundamental science, and information on the next energy scale would be hugely beneficial for the planning of future experiments. Hence, higher-precision measurements of $M_W$ are motivated.

Following the discovery of the $W$ boson in 1983 at the UA1 and UA2 experiments [7], $M_W$ has been measured with increasing precision at both lepton and hadron colliders; using $p\bar{p}$ collisions at the CDF [8–10] and D0 [11–13] experiments (Tevatron Run I and Run II), $e^+e^-$ collisions at the ALEPH [14], DELPHI [15], L3 [16], and OPAL [17] experiments (LEP), and $pp$ collisions at the ATLAS [18] experiment (LHC). The LEP and Tevatron average is $M_W = 80385 \pm 15\ \mathrm{MeV}/c^2$ [19, 20].

With the steady improvement in the experimental precision of $M_W$, the requirements for more precise theoretical and model inputs have grown. The largest source of production model uncertainty in hadron collisions is the uncertainty in the parton distribution functions. The most recent measurements from the ATLAS, CDF and D0 experiments quote the PDF-induced uncertainty as 10 MeV, 10 MeV and 11 MeV respectively, which is correlated among the measurements and dominates the total uncertainty in the world average. In this article, we explore novel methods of constraining the parton distribution functions *in situ* from the hadron collider data.

In hadron-hadron collisions, $W$ boson production can be described at the Born level via $s$-channel annihilation of quarks and antiquarks. In the $p\bar{p}$ collisions at the Tevatron, the initial-state partons are primarily valence quarks, with a smaller contribution from sea-quark annihilation. In the higher-energy $pp$ collisions at the LHC, the contribution from sea-quark annihilation is substantial. The $W$ bosons are accompanied by hadronic jets which arise from the fragmentation of radiated gluons and (anti)quarks produced by initial-state gluon splitting. The $W$ boson decays either to a quark-antiquark

pair ($q\bar{q}'$) or to a charged lepton and neutrino ($\ell\nu$). The hadronic decays cannot be used for a precise $M_W$ measurement because the jets from the $W$ boson decay cannot be calibrated to sufficient precision, and because this signal is overwhelmed by multi-jet background. The leptonic decays, $W \to \ell\nu$ ($\ell = e, \mu$), which have about 22% total branching fraction, are used for the mass measurement.

The hadron collider experiments use a coordinate system in which the $z$ axis is the axis of symmetry of the cylindrical detector and points along beam direction. Defining conventional units with $\hbar = c \equiv 1$, the rapidity $\zeta = -\frac{1}{2}\ln(E+p_z)/(E-p_z)$ is additive under boosts along the $z$ axis. In the case of massless particles, $\zeta$ equals the pseudorapidity $\eta = -\ln[\tan(\theta/2)]$, where $\theta$ is the polar angle with respect to the $z$ axis. Transverse quantities such as transverse momentum $\vec{p}_T$ are projections onto the plane perpendicular to the $z$ axis. The transverse momentum of the beam particles is considered negligible. From $\vec{p}_T$ conservation, the transverse momentum of the neutrino in $W$-boson decay is inferred as $\vec{p}_T^{\,\nu} \equiv -\vec{p}_T^{\,\ell} - \vec{u}_T$, where $\vec{p}_T^{\,\ell}$ is the transverse momentum of the charged lepton and $\vec{u}_T$ denotes the measurement of the transverse momentum of all particles recoiling against the $W$ boson.

At a hadron collider, the longitudinal momentum $p_z$ of a given $W$ boson is not measureable because beam remnants are scattered very close to the beam axis, carrying an unknown amount of longitudinal momentum. The $p_z$ distribution of the $W$ bosons is predicted by convolving the $p_z$ distributions of the interacting partons. The latter are provided by the parton distribution functions (PDFs) describing the fraction $x_i$ of a hadron's momentum carried by a given interacting parton.

Since the neutrino $p_z$ is unmeasured, $M_W$ is measured by fitting three transverse quantities: $p_T^\ell$, $p_T^\nu$, and the transverse mass $m_T = \sqrt{2p_T^\ell p_T^\nu(1-\cos\Delta\phi)}$ [21], where $\Delta\phi$ is the azimuthal angle between the charged lepton and neutrino momenta. Events are selected with $u_T \ll p_T^\ell$, so that $p_T^\ell \approx p_T^\nu$ and the Jacobian edge in the fitted distributions is not significantly smeared by the boson's transverse boost [22].

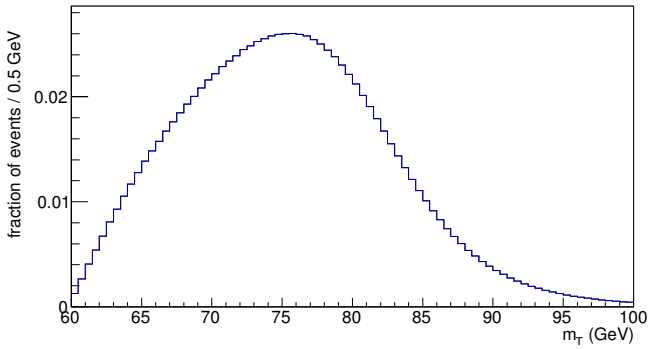


FIG. 1: The observable $m_T$ distribution from simulation.

A parametrized Monte Carlo detector simulation is used to process generator-level events in order to model the observed line shapes of the $p_T^\ell$, $p_T^\nu$, and $m_T$ distributions. The simulated $m_T$ distribution is shown in Fig. 1. Templates of these distributions are produced from the simulated events at fixed input values of the boson mass and a fixed PDF set. Additional simulated events are used as pseudo-data in which the input PDFs are varied. The templates are normalized to the pseudo-data and a maximum-likelihood fit is used to extract the observable $M_W$ corresponding to each set of PDFs. We consider the PDF parametrizations from the CTEQ [23], MSTW/MMHT [24] and NNPDF [25] collaborations.

The $p_z$ of the $W$ boson should not affect the fit to the distributions of the transverse kinematics which should be invariant under longitudinal boosts. This invariance is destroyed by the limited acceptance for the charged lepton, which is approximately $|\eta_\ell| < 1$ at the Tevatron and $|\eta_\ell| < 2.5$ at the LHC. The effect of this limited acceptance in the laboratory frame is best understood in the rest frame of the $W$ boson, where the decay polar angle $\theta^*$ determines $p_T^\ell = m_W \sin\theta_\ell^*$. Thus, events with large $p_T^\ell$ are the ones in which the $W$ boson decays centrally in the rest frame, while the events with small $p_T^\ell$ are the ones in which the decay leptons are produced in the forward-backward direction in the rest frame. Equivalently, the low $p_T^\ell$ events correspond to large $|\eta_\ell^*|$ and vice-versa.

The mapping from the rest-frame $|\eta_\ell^*|$ to the laboratory-frame $|\eta_\ell|$ is determined by the longitudinal boost of the $W$ boson and hence by the PDFs. The result of the $M_W$ fit depends on the fraction of events with low and high $p_T^\ell$, and hence the fraction of events with high and low $|\eta_\ell^*|$ respectively, that enter the $|\eta_\ell| < 1(2.5)$ acceptance of the Tevatron (LHC) detector. This ratio of events varies with PDF and captures the most important aspect of the PDF variation that induces the systematic uncertainty in the $M_W$ measurement.

The CTEQ and MSTW collaborations determine a set of eigenvectors in PDF parameter space to form an orthogonal basis. The PDF uncertainty is obtained from a quadrature sum of all eigenvector contributions in a given PDF set, $\delta M_W^{\rm PDF} = \frac{1}{2}\sqrt{\sum_i (M_W^{i+} - M_W^{i-})^2}$, where $M_W^{i\pm}$ represents the fitted mass obtained using the $\pm\sigma$ shifts in the $i^{\rm th}$ eigenvector. When the $M_W$ deviations have the same sign, half the maximum deviation between the nominal $M_W$ and $M_W^{i+}$ or $M_W^{i-}$ is used as the contribution from this eigenvector. For the NNPDF set, the $M_W$ uncertainty is given by the *rms* of the fitted $M_W$ values resulting from the 100 PDF replicas.

Using events generated with PYTHIA [26], we study the variation in the shape of the $m_T$ distribution due to the different PDF eigenvectors in a given set. We select simulated events passing the following kinematic requirements: $p_T^\ell > 30$ GeV, $p_T^\nu > 30$ GeV, $u_T < 15$ GeV and $|\eta_\ell| < 1$. For each PDF eigenvector, we normalize the $m_T$ distribution to unit area and subtract from it the normalized $m_T$ distribution corresponding to the default PDF for that set. These residual differences are shown for the CT10 and CT10W (both providing 90% confidence level (CL) uncertainties), MSTW2008 (68% CL and 90% CL), MMHT2014 (68% CL) and NNPDF3.0 PDF sets in Fig. 2. The residuals for the PDF sets which provide 90% CL uncertainties have been scaled down in order to compare to the others with 68% CL uncertainties. The NNPDF3.0 residuals have been scaled down by a factor of

10 so that the variances may be summed rather than averaged over the replicas, providing a correspondence with the sum over eigenvectors for the other PDF sets.

The pattern of the residuals as a function of $m_T$ reveals a number of features. The difference of normalized distributions must integrate to zero, requiring the presence of at least one node. Furthermore, as the $m_T$ distributions vanish near the bounds of the histogram, the residuals must also vanish near the bounds. The two striking and unexpected features are that the pattern of residuals shows only one node, and that the position of the node is almost universal for all PDF sets and all eigenvectors / replicas within a given PDF set.

Figure 2 shows that the salient feature of all PDF variations is simply to induce a variation in the fraction of events above and below a common threshold at $m_T \approx 73$ GeV. The threshold value depends on kinematic requirements and the chosen domain [60, 100] GeV of the $m_T$ histogram. The same feature is also observed in the residuals of the $p_T^\ell$ and $p_T^\nu$ distributions, indicating the universality of the underlying mechanism. This is the first important conclusion of this paper.

As the shapes of all residual distributions are very similar, the variation between eigenvectors is captured by the ratio $r = I_a/I_b$ where $I_a$ ($I_b$) represents the integral of the normalized $m_T$ distribution above (below) the threshold value of 73 GeV. The PDF variation parameter $\delta_i^J$ for eigenvector $i$ in PDF set $J$ is defined as $\delta_i^J = r_i^J - r_0^J$, where $r_0$ is computed for the default (central) PDF in the set $J$. Simultaneously, we compute the shift $\Delta_i^J = M_W(i) - M_W(0)$, where $M_W(i)$ and $M_W(0)$ refer to the fitted $M_W$ from pseudo-data generated with eigenvector $i$ and with the central PDF, respectively. As shown in Fig. 3, there is almost perfect correlation between $\delta_i^J$ and $\Delta_i^J$, indicating that the PDF systematic uncertainty in the measurement of $M_W$ is driven almost entirely by the $\delta_i^J$ observable. This is the second important conclusion of this paper.

The universality of the variation in the transverse kinematic distributions induced by the PDF parameter variations may be understood as follows. In the boson rest frame, $m_T = M_W \sin\theta_\ell^*$, in the approximation that the boson has small transverse boost. The pseudorapidity difference between the leptons with low and high $m_T$ respectively may be estimated using the relation $\sin\theta_\ell = \mathrm{sech}\,\eta_\ell$. The typical $m_T$ variation is $\approx 7.3$ GeV about the 73 GeV threshold, implying the typical values of $|\eta_\ell^*| = 0.65$ ($\eta_\ell^* = 0$) for the low (high) $m_T$ subsamples. In the absence of any boson longitudinal boost, both the low-$m_T$ and high-$m_T$ sub-samples would be fully contained within the detector acceptance $|\eta_\ell| < \eta_{\rm cut}$, where $\eta_{\rm cut}$ is 1.0 (2.5) at the Tevatron (LHC). However, the typical boson boost $y_W$ causes the preferential loss of low-$m_T$ (high $|\eta_\ell^*|$) events, when $0.65 + y_W > \eta_{\rm cut}$. At the Tevatron (LHC), events with $y_W > 0.35(1.85)$ will be preferentially lost from the low-$m_T$ sub-sample, and the PDF-induced variation in the rate of high-$y_W$ events ultimately causes the $m_W$ uncertainty.

The energy of the collider and the rapidity-acceptance of the detector work in opposite directions with regards to the sensitivity to the $y_W$ distribution. The higher the energy of the collider, the wider the actual $y_W$ distribution. The rapidity plateau for $W$ bosons extends to $y_W \approx 1.5(3.5)$ at the Tevatron (LHC). A given lepton-rapidity acceptance therefore sculpts

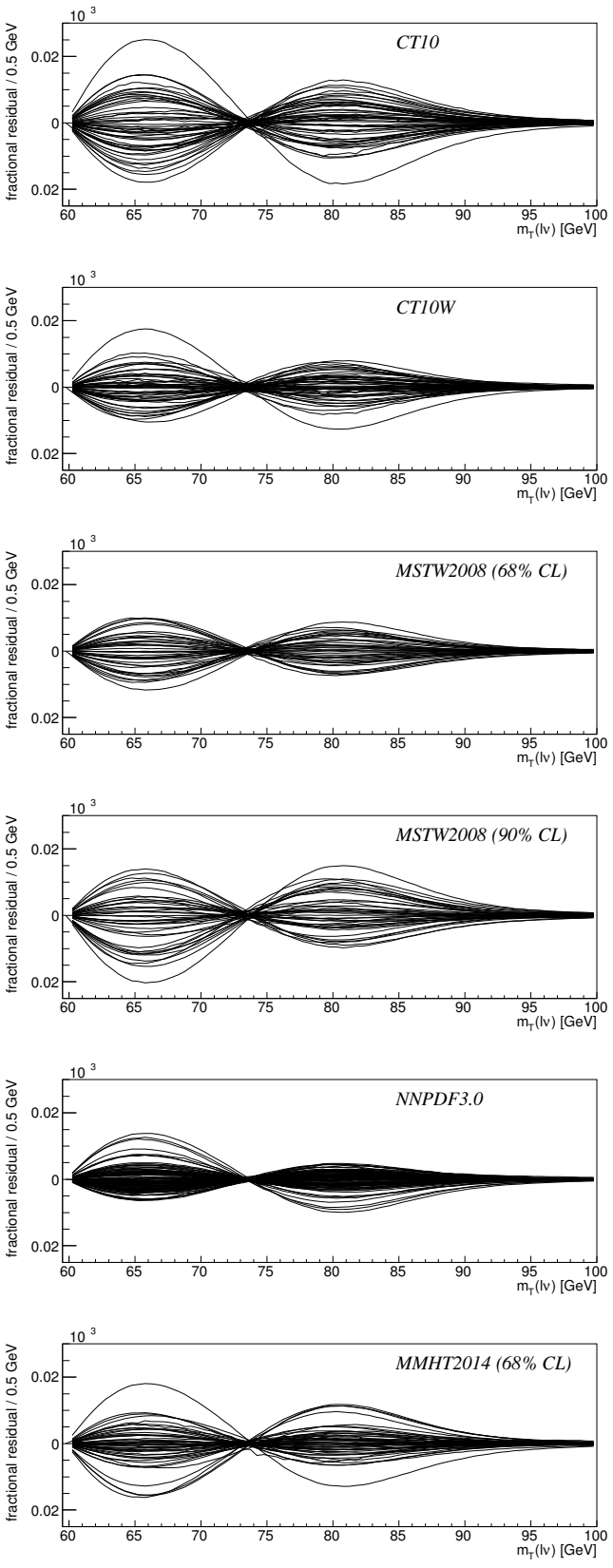


FIG. 2: Residual differences between the normalized $m_T$ distributions for six PDF sets. For each PDF set, the residuals from the default PDF are overlaid for all eigenvectors. In the case of the NNPDF3.0 set, the residuals for the 100 replicas are shown.

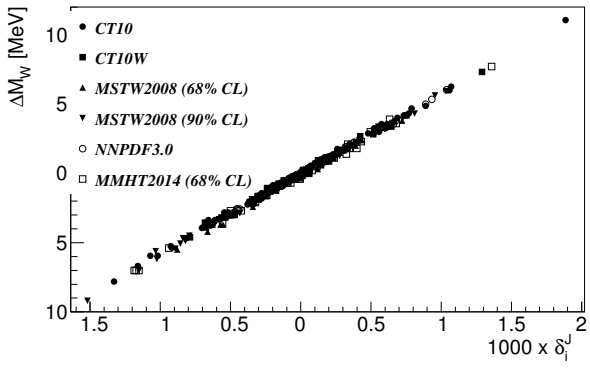


FIG. 3: Correlation between the $m_T$ distribution shape variation parameter $\delta_i^J$ and the $M_W$ shift $\Delta_i^J$, for all eigenvectors $i$ and PDF sets $J$. In the case of the NNPDF3.0 PDF set, $i$ denotes the replica index. The scale factors described in the text have been applied as for Fig. 2.

the observed rapidity and $p_T$ distributions more heavily and increases the sensitivity to the PDFs. On the other hand, at a given collider energy, a greater lepton-rapidity coverage increases the minimum $y_W$ needed to influence the low-$m_T$ subsample, thus reducing the fraction of events affected by the acceptance cut. Hence, as expected, increasing the lepton rapidity coverage reduces the sensitivity to the PDFs.

For a given collider energy and lepton acceptance, we can use $y_W \approx 0.65$ as an estimate of the boson boost differential between the low-$m_T$ and high-$m_T$ sub-samples in order to analyze the PDF sensitivity, with the understanding that the collider energy and detector acceptance will determine its typical value in a specific experiment. As we see below, the PDF sensitivity depends quadratically on the boson boost differential. Therefore, there is motivation to increase the lepton rapidity coverage such that $\eta_{\rm cut}$ approaches the width of the $W$ boson rapidity plateau and the boost differential reduces.

The $W$ boson's longitudinal kinematics are related to the momentum fractions $x_{1,2}$ of the interacting partons by $E(x_1 - x_2) = p_z^W = M_W \sinh y_W$ and $E_W = E(x_1 + x_2)$, where $E$ is the hadron beam energy, and $p_z^W$ and $E_W$ denote the longitudinal momentum and energy respectively of the $W$ boson. The labels $1(2)$ refer to the hadron moving in the positive (negative) $z$ direction. The boson's rapidity $y_W = \frac{1}{2}\ln\frac{E_W + p_z^W}{E_W - p_z^W}$ reduces to $y_W = \frac{1}{2}(\ln x_1 - \ln x_2)$. Defining $\bar{x} = M_W/(2E)$ as the partonic momentum fraction corresponding to $W$ bosons produced at rest, we find $y_W = \ln x_1 - \ln \bar{x} = \Delta \ln x$. Thus, the high $m_T$ subsample is generated from partons whose $x$ values are close to $\bar{x}$, and the low $m_T$ sub-sample is generated from partons whose $x$ values vary from $\bar{x}$ by the ratio $e^{0.65} \sim 2$, in the test case where the observed lepton has $|\eta_\ell| \approx 0$.

As the production rate is proportional to the product of PDFs $f(x_1)\cdot f(x_2)$, one finds $I_a \propto f^2(\bar{x})$ and $I_b \propto f(2\bar{x})\cdot f(\bar{x}/2)$. Defining $\xi = \ln x$ and $p(\xi) = \ln f(x)$ yields $\ln r \simeq 2p(\bar{\xi}) - p(\bar{\xi} + \Delta\xi) - p(\bar{\xi} - \Delta\xi) \approx -\partial^2 p/\partial\xi^2 \cdot (\Delta\xi)^2$, where $\Delta\xi \approx 0.65$. Therefore, the PDF variation induced in $\ln r$, which is given by $\delta_i^J$, is characterized by the variation of the second derivative of $p$ with respect to $\xi$, scaled by $(\Delta\xi)^2$.

The PDFs $p(\xi)$ are smooth functions which can be expanded in the vicinity of $\bar{\xi}$ as the Taylor expansion $p(\xi) = \Sigma_n p^{(n)}(\bar{\xi})(\Delta\xi)^n/n!$, where $p^{(n)}$ denotes the $n^{\rm th}$ derivative with respect to $\xi$. The first term representing the overall normalization of the PDF is irrelevant for the shape variable $r$ and the shape fit for $M_W$. These shape variables are also insensitive to the first derivative, which leaves the parton luminosity product $f(x_1)\cdot f(x_2)$ invariant. By extension, all odd derivatives of $p$ would leave the shape variables invariant. Thus the first relevant derivative is $p^{(2)}$, followed by $p^{(4)}$. Over the relevant $\xi$ interval with small width of $\mathcal{O}(\Delta\xi)$, the PDF variation would be dominated by the variation in a single parameter, $p^{(2)}$.

Any significant contribution from $p^{(4)}$ would be visible in Fig. 2 as a shift in the nodal point or as the presence of an additional node in the residual distribution. The absence of these features indicates that the contribution from $p^{(4)}$ and higher derivatives is substantially smaller than the dominant contribution from $p^{(2)}$.

We note that the dominant $x$-dependence of PDFs at low $x$ is given by $f(x) \sim x^{-\alpha}$, yielding $p^{(1)} = -\alpha$ and $p^{(2)} = 0$. Thus, there is no uncertainty induced in $r$ and the $M_W$ measurement by the uncertainty in $\alpha$. By isolating $p^{(2)}$ as the relevant PDF parameter, the universality of the PDF-induced uncertainty in $r$ and $M_W$ is understood. Furthermore, we obtain the insight that the PDF-induced uncertainty is caused by the variation in the sub-leading terms of the PDF parameterization at low $x$. This is the third important conclusion of this paper.

Figure 3 prompts the development of two strategies to reduce the PDF uncertainty in the measurement of the $W$ boson mass. First, a direct measurement of the ratio $r$ from the collider data can be used to constrain the PDF-induced variation in $\delta_i^J$, which will directly translate into a reduced uncertainty in $M_W$. As seen in Fig. 3, a measurement of $r$ at the level of 0.1% precision would be required. Achieving this statistical error requires in excess of two million candidate events. The full Tevatron dataset has surpassed this level of statistics, and the LHC datasets are already substantially larger and growing. A strength of this method is that the observable $r$, being a ratio of the number of events in two kinematic ranges, is not sensitive to overall normalization uncertainties such as the integrated luminosity and global efficiencies. The systematic uncertainties affecting the $r$ measurement include the kinematics-dependent background contamination and the lepton identification efficiency. More than one million $Z$-boson candidate events would be required to measure the $p_T$-dependent lepton efficiencies.

The second approach to reduce the PDF-induced systematic uncertainty is to restrict the kinematic range of the sample used for fitting [27]. Figure 4 shows the reduction in the PDF-induced uncertainty as the lower edge $L$ of the fitting window $[L, 90]$ GeV is raised from 60 GeV to 75 GeV. The reduction in the uncertainty is substantial as the variation in $\delta_i^J$ is progressively limited by the restricted domain. This is the fourth important conclusion of this paper. The reduction by the factor of two in the PDF-induced uncertainty would significantly

improve the promise of future $M_W$ measurements.

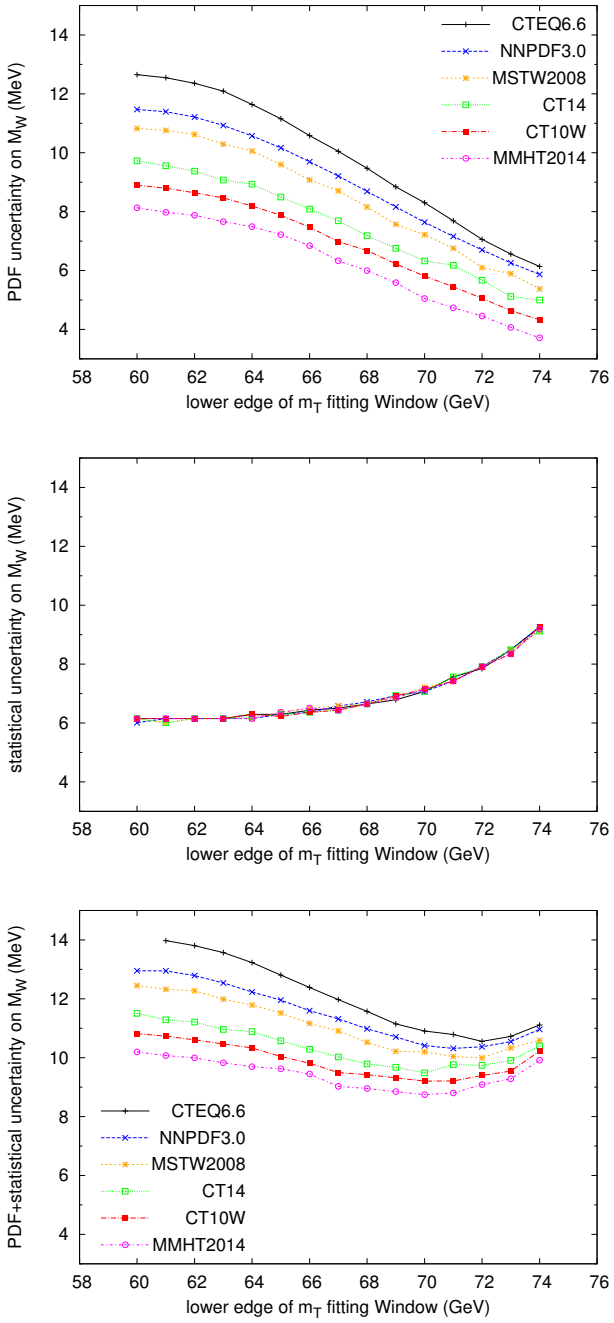


FIG. 4: The PDF-induced $M_W$ uncertainty (top), the $M_W$ statistical error (middle) and their combination in quadrature (bottom) as a function of the lower edge of the $m_T$ fitting window.

As the fitting domain is restricted, there is a corresponding loss of statistical precision in the fit. The tradeoff between the decreasing PDF uncertainty and the increasing statistical error is investigated in Fig. 4 for a sample of four million $W$ boson events. The combination in quadrature of the PDF-induced uncertainty and the statistical error is also shown in Fig. 4, illustrating the opportunity for minimizing the total uncertainty in the measurement by a judicious choice of $L$. As the sample statistics increase, raising the value of $L$ is motivated.

In summary, we have identified the salient feature of PDF variation that induces the uncertainty $\delta M_W^{\rm PDF}$ in the measurement of the $W$-boson mass. We have shown how the PDF-induced variation in the $m_T$ distribution can be characterized by a single, observable shape parameter, whose precise measurement directly translates into a reduction in $\delta M_W^{\rm PDF}$. We have also shown that $\delta M_W^{\rm PDF}$ may be reduced substantially by a judicious choice of the kinematic-fitting window, and optimized with respect to the statistical uncertainty of the fit. These methods pave the way for higher-precision $M_W$ measurements at hadron colliders.

We thank Sourav Sen for his help in accessing the PDF library. We thank Pavel Murat, Christopher Hays, Konstantinos Vellidis, Bodhitha Jayatilaka, William Ashmanskas, Willis Sakumoto, David Toback and colleagues on the CDF experiment for helpful discussions. We thank Fermilab for providing the computing resources. This work was supported by the U.S. Department of Energy.

[1] G. Aad *et al.* (ATLAS Collaboration), Phys. Lett. B **716**, 1 (2012); S. Chatrchyan *et al.* (CMS Collaboration), Phys. Lett. B **716**, 30 (2012).

[2] P. W. Anderson, Phys. Rev. **130**, 439 (1960); F. Englert and R. Brout, Phys. Rev. Lett. **13**, 321 (1964); P. W. Higgs, Phys. Rev. Lett. **13**, 508 (1964); G. S. Guralnik, C. R. Hagen, and T. W. B.

Kibble, Phys. Rev. Lett. **13**, 585 (1964).
[3] S. Glashow, Nucl. Phys. **22**, 579 (1961); A. Salam and J. C. Ward, Phys. Lett. **13**, 168 (1964); S. Weinberg, Phys. Rev. Lett. **19**, 1264 (1967).
[4] A. Sirlin, Phys. Rev. D **22**, 971 (1980).
[5] K. Nakamura *et al.* (Particle Data Group), J. Phys. G **37**, 075021 (2010).
[6] M. Ciuchini, E. Franco, S. Mishima, and L. Silvestrini, J. High Energy Phys. 08 (2013) 106; M. Baak, M. Goebel, J. Haller, A. Hoecker, D. Kennedy, K. Mönig, M. Schott, and J. Stelzer (The Gfitter Group), Eur. Phys. J. C **72**, 2003 (2012); M. Baak, M. Goebel, J. Haller, A. Hoecker, D. Kennedy, R. Kogler, K. Mönig, M. Schott, and J. Stelzer (GFitter Collaboration), Eur. Phys. J. C **72**, 2205 (2012).
[7] G. Arnison *et al.* (UA1 Collaboration), Phys. Lett. B **122**, 103 (1983); M. Banner *et al.* (UA2 Collaboration), Phys. Lett. B **122**, 476 (1983); G. Arnison *et al.* (UA1 Collaboration), Phys. Lett. B **126**, 398 (1983); P. Bagnaia *et al.* (UA2 Collaboration), Phys. Lett. B **129**, 130 (1983).
[8] T. Affolder *et al.* (CDF Collaboration), Phys. Rev. D **64**, 052001 (2001).
[9] T. Aaltonen *et al.* (CDF Collaboration), Phys. Rev. Lett. **99**, 151801 (2007); T. Aaltonen *et al.* (CDF Collaboration), Phys. Rev. D **77**, 112001 (2008).
[10] T. Aaltonen *et al.* (CDF Collaboration), Phys. Rev. Lett. **108**, 151803 (2012); T. A. Aaltonen *et al.* [CDF Collaboration], Phys. Rev. D **89**, no. 7, 072003 (2014)
[11] V. M. Abazov *et al.* (D0 Collaboration), Phys. Rev. D **66**, 012001 (2002); B. Abbott *et al.* [D0 Collaboration], Phys. Rev. Lett. **84**, 222 (2000); B. Abbott *et al.* (D0 Collaboration), Phys. Rev. D **62**, 092006 (2000); B. Abbott *et al.* (D0 Collaboration), Phys. Rev. D **58**, 092003 (1998).
[12] V. M. Abazov *et al.* (D0 Collaboration), Phys. Rev. Lett. **103**, 141801 (2009).
[13] V. M. Abazov *et al.* (D0 Collaboration), Phys. Rev. Lett. **108**, 151804 (2012); V. M. Abazov *et al.* [D0 Collaboration], Phys. Rev. D **89**, no. 1, 012005 (2014).
[14] S. Schael *et al.* (ALEPH Collaboration), Eur. Phys. Jour. C **47**, 309 (2006).
[15] J. Abdallah *et al.* (DELPHI Collaboration), Eur. Phys. Jour. C **55**, 1 (2008).
[16] P. Achard *et al.* (L3 Collaboration), Eur. Phys. Jour. C **45**, 569 (2006).
[17] G. Abbiendi *et al.* (OPAL Collaboration), Eur. Phys. Jour. C **45**, 307 (2006).
[18] M. Aaboud *et al.* [ATLAS Collaboration], Eur. Phys. Jour. C **78**, 110 (2018).
[19] ALEPH, CDF, D0, DELPHI, L3, OPAL, and SLD Collaborations, the LEP Electroweak Working Group, the Tevatron Electroweak Working Group, and the SLD Electroweak and Heavy Flavour Groups, CERN Report No. CERN-PH-EP-2010-095, and Fermilab Report No. FERMILAB-TM-2480-PPD, 2010
[20] T. Aaltonen *et al.* (CDF and D0 Collaborations), Phys. Rev. D **88**, 052018 (2013).
[21] J. Smith, W. L. van Neerven, and J. A. M. Vermaseren, Phys. Rev. Lett. **50**, 1738 (1983).
[22] Y. Zeng, Ph.D. thesis, Duke University (2012), FERMILAB-THESIS-2012-27.
[23] J. Pumplin, D.Stump, J. Huston, H. Lai, P. Nadolsky, and W. Tung, J. High Energy Phys. 0207, 012 (2002); P. Nadolsky, H. Lai, Q. Cao, J. Huston, J. Pumplin, D. Stump, W. Tung, and C.-P. Yuan, Phys. Rev. D **78**, 013004 (2008); S. Dulat *et al.*, Phys. Rev. D **93**, no. 3, 033006 (2016).
[24] A. D. Martin, W. J. Sirling, R. S. Thorne, and G. Watt, Eur. Phys. J. C **63**, 189 (2009); L. A. Harland-Lang, A. D. Martin, P. Motylinski, and R. S. Thorne, Eur. Phys. J. C **75**, 204 (2015).
[25] R. D. Ball *et al.* [NNPDF Collaboration], Eur. Phys. J. C **77**, no. 10, 663 (2017); R. D. Ball *et al.* [NNPDF Collaboration], JHEP **1504**, 040 (2015).
[26] T. Sjöstrand, Comput. Phys. Commun. **82**, 74 (1994). We use version 6.129 for $W$ and $Z$ production, version 6.136 for $\Upsilon$ production, and version 6.157 for $J/\psi$ production.
[27] The same conclusion has been reached independently by Christopher Hays, Oxford University, in a private communication.